Exploring the evolution and adaptive role of mosaic aneuploidy in a clonal *Leishmania donovani* population using high throughput single cell genome sequencing

Gabriel H. Negreira[1], Pieter Monsieurs[1], Hideo Imamura[1], Ilse Maes[1], Nada Kuk[2], Akila Yagoubat[2], Frederik Van den Broeck[1], Yvon Sterkers[2], Jean-Claude Dujardin[1,3], Malgorzata A. Domagalska[1]

Authors Affiliation:

[1] Institute of Tropical Medicine Antwerp, Molecular Parasitology Unit, Antwerp, Belgium

[2] Université Montpellier, UFR Médecine, Laboratoire de Parasitologie-Mycologie, Montpellier, France

[3] University of Antwerp, Department of Biomedical Sciences, Antwerp, Belgium.

Keywords: Leishmania, single cell genomic sequencing, mosaicism, aneuploidy

Abstract

Maintenance of stable ploidy over continuous mitotic events is a paradigm for most higher eukaryotes. Defects in chromosome segregation and/or replication can lead to aneuploidy, a condition often considered deleterious. However, in *Leishmania,* a Protozoan parasite, aneuploidy is a constitutive feature, where variations of somies represent a mechanism of gene expression adaptation, possibly impacting phenotypes. Strikingly, clonal *Leishmania* populations display cell-to-cell somy variation, a phenomenon named mosaic aneuploidy (MA). However, until recently, no method was available for the determination of the complete karyotype of single *Leishmania* parasites. To overcome this limitation, we used here for the first time a high-throughput single-cell genomic sequencing (SCGS) method to estimate individual karyotypes of 1560 promastigote cells in a clonal population of *Leishmania donovani*. We identified 128 different karyotypes, of which 4 were dominant. A network analysis revealed that most karyotypes are linked to each other by changes in copy number of a single chromosome and allowed us to propose a hypothesis of MA evolution. Moreover, aneuploidy patterns that were previously described by Bulk Genome Sequencing as emerging during first contact of promastigotes populations with different drugs are already pre-existing in single karyotypes in the SCGS data, suggesting a (pre-)adaptive role of MA. Additionally, the degree of somy variation was chromosome-specific. The SCGS also revealed a small fraction of cells where one or more chromosomes were nullisomic. Together, these results demonstrate the power of SCGS to resolve sub-clonal karyotype heterogeneity in *Leishmania* and pave the way for understanding the role of MA in these parasites' adaptability.

36 **Introduction**

37 Historically, cell populations were analyzed in bulk assuming that this provides the
38 representative information on the biology and behavior of these cells in a given experimental
39 set up. The existence of heterogeneity between single cells, even in clonal populations, has
40 been acknowledged but for long it was not further explored due to lack of suitable
41 methodologies, and also because of the assumption that this cell-to-cell variation is random
42 and has no biological significance. In the last years, advances in single cell imaging, molecular
43 biology and systems biology enabled analysis and quantification of differences between single
44 cells, defining new cell types and their origin, and finally allowing the demonstration of
45 functional relevance of this variation[1]. This cell-to-cell variability of clonal populations is also of
46 essential importance for unicellular organisms, like *Staphylococcus aureus*[2] , or *Sacharomyces*
47 *cerevisiae*[3]. Similarly, for digenetic protozoan parasites, such as *Plasmodium spp*. or
48 *Trypanosoma cruzi*, cellular mosaicism was also demonstrated to be crucial for drug resistance
49 or tissue tropism during the vertebrate host infection[4].

50 *Leishmania* sp. are digenetic unicellular protozoan parasites responsible for a spectrum
51 of clinical forms of leishmaniasis worldwide and causing 0.7-1 million new cases per year[5]. As
52 other trypanosomatids, *Leishmania* belongs to the supergroup Excavata, one of the earliest
53 diverging branch in the Eukaryota domain[6]. Thus, several molecular mechanisms considered
54 canonical for eukaryotes are different in these parasites, including the genomic organization in
55 long polycistronic units, the near absence of transcription initiation regulation by RNA
56 polymerase II promoters with gene expression regulation happening mostly through post-
57 transcriptional mechanisms[7], and its remarkable genomic plasticity[8]. The genome of *Leishmania*
58 sp is ubiquitously aneuploid, and high levels of chromosomal somy variation, as well as local
59 gene copy number variation are found between all *Leishmania* species[9,10]. Moreover, these
60 variations are highly dynamic and change in response to new environment, such as drug
61 pressure, vertebrate host or insect vector[11]. Changes in somy, together with episomal gene
62 amplifications, and not variation in nucleotide sequence are the first genomic modifications
63 observed at populational level during the course of experimental selection of drug resistance,
64 suggesting that they are adaptive[12,13]. Importantly, somy alterations are reflected in the level
65 of transcriptome[11], and -for a same life stage- to a great degree of proteome derived from genes
66 located in polysomic chromosomes[14]. These findings further support the notion that *Leishmania*
67 exploits aneuploidy to alter gene dosage and to adapt to different environment.

68 Cell-to-cell variation in *Leishmania* has been so far reported in the form of mosaic
69 aneuploidy (MA). This phenomenon was demonstrated in several *Leishmania* species by means
70 of fluorescence in situ hybridization (FISH) performed on a few chromosomes, which showed
71 at least two somy states among individual cells[15]. As a consequence, thousands of different
72 karyotypes are expected to co-exist in a parasite population[16]. This heterogeneity of aneuploidy
73 provides a huge potential to generate diversity in *Leishmania* from a single parental cell, both
74 quantitatively through gene dosage, but also qualitatively through changes in heterozygosity[17].
75 Thus, it is hypothesized that mosaic aneuploidy constitutes a unique source of adaptability to
76 new environment for the whole population of parasites[16].

77 Although MA has been demonstrated by FISH, its extent to all over the 35-36
78 chromosomes of *Leishmania*, its dynamics in constant as well as new environment and its
79 potential role in adaptation to different environment remains to be determined. Accordingly,
80 pioneer FISH-based studies should be complemented and refined by single cell genome
81 sequencing (SCGS). In a previous study[18], we made a first step in that direction by combining
82 FACS-based sorting of single *Leishmania* cells with whole genome amplification (WGA) and
83 whole genomic sequencing (WGS). In this pilot study, we evaluated different WGA and
84 bioinformatic methods and detected 3 different karyotypes among 28 single cells of *L.*
85 *braziliensis*[18]. Here, we made one step beyond, applying a droplet-based platform for single cell
86 genomics, in order to undertake the first high-throughput study of MA in *Leishmania*.

87 **Material and Methods**

88 **Parasites**

89 *L. donovani* promastigotes of the strain MHOM/NP/03/BPK282/0 clone 4 (further called
90 BPK282, reference genome of *L. donovani*) were maintained at 26˚C on HOMEM medium
91 (Gibco, ThermoFisher) supplemented with 20% Fetal Bovine Serum, with regular passages done
92 every 7 days. The strain was submitted to SCGS 21 passages after cell cloning and analyzed by
93 FISH 23 passages later.

94 **Cell Suspension Preparation for SCGS**

95 BPK282 promastigotes at early stationary phase (day 5) were harvested by centrifugation
96 at 1000rcf for 5 minutes, washed twice with PBS1X (without calcium and magnesium) + 0,04%
97 BSA, diluted to $5x10^6$ parasites/mL and passed through a 5µm strainer to remove clumps of
98 cells. After straining, volume was adjusted with PBS1X + 0,04% BSA to achieve a final
99 concentration of $3x10^6$ parasites/mL. The absence of remaining cell duplets or clumps in the
100 cell suspension was confirmed by microscopy.

101 **Single Cell partitioning, barcoding, WGA and sequencing**

102 We used 4.2µL of the single-cell suspension as input to the 10X Chromium™ Single Cell CNV
103 Solution protocol (10X Genomics), targeting a total of 2000 sequenced cells according to the
104 manufacturer's instructions. Individual cells were portioned and incapsulated in a hydrogel
105 matrix using a microfluidic chip and the Chromium Controller (10X Genomics). During cell
106 partitioning, each cell was combined with the Cell Bead (CB) Polymer™ and the Cell Matrix™
107 reagents, forming the CBs. CBs were then incubated overnight at 21˚C and 1000RPM on a
108 thermomixer for homogeneous hardening of the CB polymer. The individually incapsulated cells
109 were lysed, releasing the genomic DNA (gDNA) inside the CB. In a second microfluidic chip, each
110 CB was individually joined with a Gel Bead (GB) containing multiple copies of one of the
111 ~750.000 unique 10X barcodes™, together with an enzyme mix used in downstream Whole
112 Genome Amplification (WGA) and ligation of 10X barcodes. The CB-GB joining was performed
113 with a partitioning oil, forming an emulsion where each droplet (GEMs) contain a single CB
114 linked to a unique GB. Inside the GEMs, the CB and GB were disrupted, and isothermal WGA
115 with random hexamers followed by ligation of the 10X barcode to the amplified gDNA
116 molecules was carried out. Then, GEMs were disrupted, amplified DNA molecules were pooled
117 and processed for Illumina sequencing with the addition of P5 and P7 adaptors and a sample

118 index. Sequencing of the library was performed at Genomics Core Leuven (Belgium), with a
119 NextSeq High Output kit (Illumina) platform with 2 x 150 read length.

120 **CNV Calling and Somy Estimation**

121 Reads were associated to each sequenced cell based on their 10X-barcode sequence and
122 mapped to a customized version of the reference *L. donovani* genome LdBPKv2[11] (available at
123 ftp://ftp.sanger.ac.uk/pub/project/pathogens/Leishmania/donovani/LdBPKPAC2016beta/),
124 where Ns were added to the ends of chromosomes 1 to 5 to reach the 500kb minimum size
125 allowed by the Cell Ranger DNA™ pipeline (10X Genomics). The normalized read depth (NRD)
126 within adjacent, non-overlapping 80kb bins was used to calculate copy number values (referred
127 here as CNV values) in 80kb intervals, using the version 1.1 of the Cell Ranger DNA™ pipeline[19].
128 CNV values represent the integer NRD of each bin after scaling of NRD values by the baseline
129 ploidy factor (S factor) of each cell determined by the scaling algorithm of the pipeline[20]. We
130 used the arguments min-soft-avg-ploidy and max-soft-avg-ploidy set to 1.9 and 2.1,
131 respectively, to encourage the scaling algorithm to establish cells baseline ploidy to 2. This was
132 done to avoid overscaling artifacts generated by the scaling algorithm that were observed in
133 some cells when these options were not used. CNV values were visualized in the Loupe scDNA
134 Browser (10X Genomics)[21], with cells arranged in 512 clusters, the maximum number of clusters
135 allowed by the software. These clusters were composed of 1 to 7 cells each that were grouped
136 together based on CNV values similarities[22]. CNV values of each 80kb bin of all 512 clusters
137 were exported as a csv file and the average CNV values of intrachromosomic bins were used to
138 estimate chromosomal somy. Bins mapping to high copy number loci such as the H-locus
139 (chromosome 23) and M-locus (chromosome 36)[23] were excluded from the calculation. Bin-to-
140 bin variability was estimated by the normalized standard deviation of CNV values of
141 intrachromosomal bins. Each cell cluster received a bin variability score based on the average
142 bin-to-bin variability of all chromosomes. Clusters displaying a bin variability score higher than
143 0.05 were excluded. Remaining clusters were ungrouped, with somy values of each individual
144 cell corresponding to the somy values estimated for their original clusters.

145 **Karyotypes identification and network analysis**

146 In order to identify different karyotypes present in the sequenced population, somy values
147 of each cell were rounded to their closest integer. Cells displaying the same rounded somy
148 values for all chromosomes were considered as having the same karyotype. Each unique

149 karyotype identified in the population received an identifier composed by the concatenated
150 rounded somy values of all chromosomes, from chromosome 1 to chromosome 36 (e.g.,
151 "222232223222222322222232232222423232"). Unique karyotypes were numerically named
152 according to their frequency in the sequenced population.

153 To perform a network analysis, a pairwise distance matrix was built based on the number
154 of different chromosomes between all karyotype and used to generate a randomized minimum
155 spanning tree with 100 randomizations, using the Pegas R package[24,25].

156 **DNA probes and fluorescence in situ hybridization (FISH)**

157 DNA probes were either cosmid (L549 specific of chromosome 1) or BAC (LB00822 and
158 LB00273 for chromosomes 5 and 22 respectively) clones that were kindly provided by Peter
159 Myler (Seattle Biomedical Research Institute) and Christiane Hertz-Fowler (Sanger Centre). DNA
160 was prepared using Qiagen Large-Construct Kit and labelled with tetramethyl-rhodamine-5-
161 dUTP (Roche Applied Sciences) by using the Nick Translation Mix (Roche Applied Sciences)
162 according to manufacturer instructions. Cells were fixed in 4% paraformaldehyde then air-dried
163 on microscope immunofluorescence slides, dehydrated in serial ethanol baths (50–100%) and
164 incubated in NP40 0,1 % for 5 min at RT. Around 100 ng of labelled DNA probe was diluted in
165 hybridization solution containing 50% formamide, 10% dextran sulfate, 2× SSPE, 250 $\mu g.mL^{-1}$
166 salmon sperm DNA. Slides were hybridized with a heat-denatured DNA probe under a sealed
167 rubber frame at 94°C for 2 min and then overnight at 37°C and sequentially washed in 50%
168 formamide/2× SSC at 37°C for 30 min, 2× SSC at 50°C for 10 min, 2× SSC at 60°C for 10 min, 4×
169 SSC at room temperature. Finally, slides were mounted in Vectashield (Vector Laboratories)
170 with DAPI. Fluorescence was visualized using appropriate filters on a Zeiss Axioplan 2
171 microscope with a 100× objective. Digital images were captured using a Photometrics CoolSnap
172 CCD camera (Roper Scientific) and processed with MetaView (Universal Imaging). Z-Stack image
173 acquisitions (15 planes of 0.25µm) were systematically performed for each cell analyzed using
174 a Piezo controller, allowing to view the nucleus in all planes and to count the total number of
175 labelled chromosomes. Around 200 cells [187-228] were analyzed per chromosome.

176 **Results**

177 In this study, we submitted the clonal population of BPK282 promastigotes to a high
178 throughput, droplet-based SCGS method (Chromium™ CNV Solution - 10X Genomics). In total,
179 148,7M reads were generated, of which 49,7M were mapped to 1703 cells after removal of
180 duplicated reads. The average effective coverage depth per cell was 0,14x, with only 2 cells
181 displaying a depth coverage higher than 1x (**Figure S1A)**. However, read mapping was evenly
182 distributed across chromosomes in general(**Figure S1B**), which allows somy estimation despite
183 low depth[18]. From 512 clusters, 452 passed the bin-to-bin variability filtering, representing a
184 total of 1560 cells. Most eliminated clusters displayed an average somy close to 1 (**Figure S1C**).

185 **Copy number variation of individual chromosomes**

186 The somies of the 36 *L. donovani* chromosomes in the 1560 filtered cells are depicted in
187 **Figure 1A**. Of these 36 chromosomes, 7 were predominantly trisomic (chromosomes 5, 9, 16,
188 23, 26, 33 and 35), while chromosome 31, the only chromosome that is extensively reported as
189 polysomic (often tetrasomic) in all *Leishmania* species studied so far[9,26], was also tetrasomic in
190 most cells in our SCGS data. The other chromosomes were mostly disomic. These observations
191 are very similar to the populational aneuploidy pattern estimated by BGS of the BPK282
192 reference strain (**Figure 1A, top heatmap, and Figure S2**). Notably, chromosome 13, which
193 display an intermediate somy value in the Bulk Genomic Sequence (BGS) data, was found as
194 disomic and trisomic at high proportions in the SCGS. Moreover, our SCGS data revealed that
195 high cell-to-cell somy variation was chromosome-specific (**Figure 1B**). For instance,
196 chromosomes 18 and 21 were disomic in 99,94% of the cells, with only one cell for each
197 displaying a different somy (**Supplementary table 1 – kar89 and kar100 respectively**).
198 Conversely, chromosomes 13, 35 and 5 were the most variable ones, where, respectively,
199 25,64%, 25,26% and 21,41% of the cells displayed a somy divergent from the most frequent
200 one.

201 In the filtered data, we identified a cell where 4 chromosomes were estimated as nullisomic
202 (**Supplementary table 1 - kar89)**. The bam file of this cell shows that these chromosomes had
203 no sequenced reads mapping to them (**Figure 2A**, first plot), indicating that they were absent in
204 this cell. An investigation of the bam files of all cells, including the ones eliminated after data
205 filtering, revealed a total of 12 cells displaying at least one chromosome with no reads mapping

206 to it, of which 11 displayed a high intrachromosomal bin-to-bin variability of the mapped
207 chromosomes and were excluded during data filtering.

208 **Karyotype mosaicism**

209 A karyotype was defined as any unique combination of rounded somy values for all
210 chromosomes identified in the sequenced cells after data filtering. According to this definition,
211 128 different karyotypes were identified amid 1560 cells. The most frequent karyotype (kar1)
212 was found in 431 cells, representing 27,65% of the sequenced population; this karyotype is
213 equivalent to the average karyotype observed by BGS of BPK282. Four karyotypes are
214 dominant in the population, representing 62,5% of cells (**Figure 3A**). Noteworthy, the most
215 dominant karyotypes displayed little somy difference between each other. For instance, kar2,
216 3 and 4 differ from kar1 by changes in somy in a single chromosome, i.e. chromosomes 13, 35
217 and 5 respectively, while kar5 diverge from kar2 by a disomy in chromosome 35 (**Figure 3B**).
218 A network analysis showed that most karyotypes diverge from another by a difference in a
219 single chromosome, displaying an interesting pattern where most karyotypes can be linked
220 back to kar1 by single chromosome-change steps (**Figure 4**, black pies). Noteworthy, kar1 also
221 displays the biggest number of secondary karyotypes directly linked to it by somy changes in
222 single chromosomes, including the other 3 dominant karyotypes. Karyotypes which the closest
223 relatives were at two or more chromosome changes apart (red pies) were only present at
224 frequencies lower than 0,44%. Moreover, the only karyotype with nullisomic chromosomes
225 that passed the data filtering criteria (kar89) display several chromosomes with somies
226 different from most karyotypes, with the closest one (kar32) being 18 chromosomes somy
227 changes apart from it.

228 **Pre-existing karyotypes selected during early environmental adaptation.**

229 Previous studies have demonstrated through BGS that *in vitro Leishmania* populations
230 display changes in average aneuploidy patterns of the cell population as one of the first genomic
231 alterations when submitted to environmental changes, including hosts infection and drug
232 pressure[11–13,27]. However, it is still unknown if these variations in somies observed at
233 populational level are generated by selection of karyotypes pre-existing in subpopulations or
234 represent *de novo* alterations induced by the new environmental pressure. To address this
235 issue, we revisited previously published BGS data where the same BPK282 clonal promastigote
236 population was used as model in drug selection experiments. We evaluated in our SCGS data if

237 changes in aneuploidy patterns that emerge during adaptation to different drug pressures at
238 populational level are already present in single karyotypes in the BPK282 population.

239 In the 3 revisited drug resistance selection studies, the same pattern was observed. First
240 rounds of selection led to changes in the average populational aneuploidy profile that were
241 equivalent to single karyotypes present in our SCGS data (**Figure 5**). Authors[13] reported a
242 reduction in the somy of chromosomes 13 and 35 in a BPK282 population exposed to 3µM and
243 6µM of Miltefosine. The observed populational aneuploidy pattern is similar to kar9, found in
244 24 cells in our SCGS data, where chromosomes 13 and 35 are disomic (**Figure 5A**). A similar
245 observation happened when BPK282 promastigotes were exposed to 2µM and 4µM of
246 Paramomycin in another study[27], where the somy changes are also similar to kar9 (**Figure 5B**).
247 Finally, *in vitro* SbIII selection experiments with BPK282 led to changes in populational average
248 somies which were similar to karyotypes 3, 4, or 6 among 3 replicates exposed to 48µM of the
249 drug [12] (**Figure 5C**). However, in these 3 studies, higher drug concentrations led to changes in
250 the average populational somies that are not represented by single karyotypes in our data.

251 **Validation of the SCGS results with FISH**

252 As a validation to our SCGS data, we also evaluated the somy of 3 chromosomes in 187-228
253 BPK282 cells using FISH. We observed very similar somies distributions in both methods (**Figure**
254 **6**). For instance, chromosome 5, the most variable of the 3 assessed chromosomes, was
255 estimated as trisomic in 78,5% of the cells in the SCGS data, and 74,5% by FISH, while it was
256 disomic in 20,9% in SCGS and 22,6% in FISH. Chromosome 1 was estimated as disomic in 94,8%
257 of the cells in the SCGS and 96,2% in FISH, with a smaller fraction of cells being monosomic
258 (5,1% in SCGS and 3,2% in FISH). Chromosome 22 had slightly more divergent values between
259 both methods, being disomic in 99,5% in SCGS and 92,1% in FISH, with a fraction of 7,9% of cells
260 that were found as monosomic in FISH while monosomy for chromosome 21 was found in only
261 0,19% of the cells in SCGS. In general, the similarities between the distributions found in both
262 methods supported the reliability of SCGS.

263 **Discussion**

264 The parallel whole genomic sequencing of 1560 *Leishmania* promastigotes reported here
265 allowed us to reveal for the first time a complex mosaicism of complete karyotypes in
266 *Leishmania* with unprecedent resolution. By estimating the somy of all 36 chromosomes in each
267 sequenced single parasite, we could determine which chromosomes were more prone to cell-
268 to-cell somy variability, which were the frequencies of each identified karyotype in the clonal
269 population and the divergencies between these karyotypes. Our data was further supported by
270 FISH, which is a well establish method for the quantification of individual chromosome copy
271 number in single *Leishmania* cells[28]. Thus, this work represents the first high throughput SCGS
272 study of MA in *Leishmania*.

273 **Performance and challenges of the SCGS method**

274 In general, the whole genome amplification (WGA) method used in the Chromium™ Single
275 Cell CNV solution seems to generate an even genome coverage, which has been demonstrated
276 as a more relevant aspect than coverage depth for accurate somy estimation[18,29]. However, a
277 low percentage of cells displaying a higher read count variability might reflect on inaccurate
278 CNV values, and therefore, unreliable karyotype determination. The Cell Ranger DNA™ pipeline
279 uses an hierarchical clustering algorithm to combine the read counts of cells with similar CNV
280 values to enhance the resolution and reliability of CNV values determination[22], thus greatly
281 reducing the number of faulty karyotypes. Yet, cells with slightly different karyotypes might be
282 clustered together due to inaccurate single-cell CNV values estimation, leading to a cluster somy
283 pattern that does not reflect a true biological karyotype. Since we noticed that artificial
284 karyotypes were caused by chromosomes with high variation in intrachromosomal CNV values,
285 we applied an addition data filtering step where we eliminated clusters displaying a high
286 intrachromosomic bin-to-bin variability. This led to the removal of 56 clusters (143 cells),
287 corresponding to 51 karyotypes. Most of the eliminated karyotype displayed somy patterns that
288 were highly distinct from the ones found in the remaining karyotypes after data filtering,
289 probably due to inaccurate somy estimation caused by the high intrachromosomic bin-to-bin
290 variability.

291 Most eliminated clusters had the majority of CNV values assigned to 1. Since CNVs are
292 calculated by the relative read depth of the bins, the Cell Ranger DNA™ pipeline uses an
293 algorithm that determines the baseline ploidy of each cell by scaling the normalized read depth

294 values of each bin by a factor S that satisfies the condition where all normalized read depth
295 values are integers multiple of S[20]. Candidate values for S are heuristically determined following
296 a rule where if the cell displays the same copy number in most of the genome, S is set to a value
297 that leads to an average ploidy close to 2, otherwise, in the presence of high variable CNV
298 values, S is determined as the lowest value that satisfies the condition mentioned above. Thus,
299 it is likely that the high variation of local CNV values present in these clusters, reflecting in a
300 high intrachromosomic bin-to-bin variability, led to an unprecise determination of the S factor
301 by the scaling algorithm, leading to an average ploidy in these clusters close 1. Indeed, the
302 software cannot identify haploid cells since it is based on a normalized read depth quantification
303 method. Haploid cells could be identified by the evaluation of heterozygous SNPs in single cells.
304 However, the read depth per cell of our data does not allow such analysis.

305 The Cell Ranger DNA™ pipeline was developed to handle mammal genomes[30]. The nuclear
306 genome of *Leishmania* is about 100 times smaller than human's, and even the biggest *L.*
307 *donovani* chromosome (Chr36, 2,768Mbp[31]) is still 17 times smaller than the smallest human
308 chromosome (Chr21, 46,7Mbp). With the 80kb bin size determined by the pipeline in this data,
309 small chromosomes such as Chr1, Chr2 and Chr3 are represented by 3 to 5 bins. However, this
310 does not seem to introduce a variability bias to small chromosomes in general, since the
311 observed cell-to-cell somy variability does not correlate to chromosome size. For instance, Chr4,
312 Chr5 and Chr6 are all represented by 6 bins, and while Chr5 was found as triploid and diploid in
313 high proportions for both states, Chr4 and Chr6 were among the less variable chromosomes
314 (**Figure 1B**). Conversely, Chr34 and Chr35 had 24 and 27 bins respectively, and while the former
315 was found as disomic in more than 95% of the cells, the later was estimated as disomic in 26,9%
316 and trisomic in 71,4% of the cells. There is the possibility, however, that the very low number
317 of bins for chromosome 1 (3 bins) introduced a bias towards monosomy.

318 On the other hand, the reduced size of *Leishmania* genome means that higher coverage
319 depth per cell are achieved with relatively lower total sequence depth. The average 29.191
320 mapped deduplicated reads per cell resulted in an average coverage depth/cell of 0,14x. For
321 human cells, the recommended 750.000 reads/cell is expected to yield a coverage depth of
322 ~0,05x/cell, allowing CNVs assessment at 2mb resolution only[32]. This means that for each bin,
323 a higher number of reads are expected in *Leishmania*, increasing CNV estimation resolution.
324 Therefore, the higher coverage depth/cell seem to compensate the lower number of bins per
325 chromosome in *Leishmania* genome.

326 **SCGS data supports errors in chromosome replication as main drivers of mosaicism**

327 In a previous FISH-based study, authors reported asymmetrical chromosome allotments
328 (ACA) in dividing nuclei as the cause of MA[15]. Remarkably, in all cells displaying ACA, the total
329 copy number of the evaluated chromosome in the daughter cells were always odd ("3+2" or
330 "2+1"). This observation suggests that mosaicism in aneuploidy is generated by defects in
331 replication of chromosomes during cell division, as discussed by the authors, and not by errors
332 in chromosome segregation, where the expected number of copies between daughter cells
333 would be even. In our SCGS data, a pairwise comparison between all karyotypes that diverged
334 from another by a single chromosome revealed that complementary karyotypes that could
335 represent mis-segregation event are very rare. Of 127 possible pairs, only 7 pairs could be
336 explained by a mis-segregation event (**Figure 7 and Supplementary table 2**). The other 120 pairs
337 displayed a "2+1", "2+3", "3+4" or "4+5" pattern in the divergent chromosome, supporting the
338 hypothesis that such karyotypes were probably generated by under- or over-replication of
339 single chromosomes during mitosis.

340 One of the effects of ACA events is the possibility of some cells losing all copies of a
341 chromosome (nullisomy). Among all 1703 cells sequenced, including the ones that were
342 removed for further analysis, 12 had one or more chromosome which was nullisomic. This
343 represents ~0,7% of the total, which is a relatively high frequency considering that an *in vitro*
344 *Leishmania* culture can consist of millions of cells. The fact that almost all cells with an absent
345 chromosome displayed a karyotype that was not similar to any other in the sequenced
346 population (**Figure S4**) is possibly due to the high bin-to-bin variability found in these cells,
347 which hampers CNV estimation. The noisy coverage of these cells could be an indicative of DNA
348 degradation after cell death, potentially caused by the lack of one or more chromosomes,
349 suggesting that nullisomy is lethal for these parasites. In this case, the relatively high rate of
350 cells with absent chromosomes is an indicative that ACA events that lead to nullisomy happen
351 at high frequencies. Indeed, the FISH analysis of dividing nuclei found that for 2 chromosomes
352 (chromosomes 2 and 22), around 1% of the evaluated parasites were displaying a "1+0"
353 distribution of chromosomes between sister nuclei in *L. major*[15].

354 **Chromosome Somy Variability**

355 Although pioneer FISH studies demonstrated that somy mosaicism was more prominent in
356 some chromosomes than others, the complete somy landscape of all chromosomes in a

357 *Leishmania* population was still unknown at single-cell level, since only 11 chromosomes were
358 evaluated by FISH hitherto. Our SCGS data revealed that some chromosomes display a
359 remarkable lack of cell-to-cell variability in the sequenced population, while others are more
360 prone to mosaicism. Several of the less variable chromosomes also display low inter-strain
361 variation between *L. donovani* isolates. For instance, chromosomes 10, 17, 18, 19, 21, 24, 25,
362 27, 28, 30, 34 and 36 were previously reported as disomic by BGS in more than 95% of 204
363 isolates in a previous study[33], and were disomic in more than 98% of the cells in our SCGS data,
364 suggesting a pressure to maintain these chromosomes as disomic, at least under standard *in*
365 *vitro* conditions. Conversely, chromosomes 5, 13, 33 and 35, the most variable in the SCGS, are
366 also present as disomic or trisomic at high proportions between these different isolates. This
367 indicates that, in a given environment, somy variability is restricted to a specific group of
368 chromosomes. One possibility is that gene contents of some chromosomes are more tolerant
369 to dosage imbalance than others, suggesting that selective pressure maintain somy stability in
370 some chromosomes while allow more plasticity in others. Moreover, the WGS of 204 *L.*
371 *donovani* isolates revealed that only chromosome 34 was consistently disomic in all strains[33].
372 However, BPK282/0 cl4 parasites displays a trisomy for this chromosome when exposed to high
373 SbIII concentrations[12], suggesting that every chromosome has the potential to became
374 polysomic depending on environmental pressures. The fact that, in our data, the karyotypes
375 that dominate the population are similar to each other while karyotypes with several somy
376 changes happen at low frequencies also suggests that selective pressure play a role in somy
377 variability.

378 **Hypothesis on the evolution of mosaic aneuploidy in the clonal BPK282 population**

379 By performing a pairwise comparison of the identified karyotypes in BPK282, we revealed a
380 network structure where most karyotypes are linked to each other by single somy changes. This
381 network allows proposing a hypothesis for the evolution of mosaicism during the 20 passages
382 that followed cellular cloning. Kar1, the most frequent in the sequenced cells, is also the one
383 displaying the highest number of karyotypes directly linked to it (**Figure 4**). Kar1 shows the same
384 aneuploidy pattern as the 'average' karyotype assessed by BGS in the uncloned BPK282/0 line[11],
385 suggesting that this was also the dominant karyotype in the parental population. The high
386 frequency of this karyotype in the parental population naturally increases the chance of it being
387 randomly picked when starting a clonal population. Altogether, these data suggest that kar1
388 was the potentially founder karyotype of the BPK282 clonal population derived from this

389 uncloned BPK282/0 line. Kar1 is likely well adapted to *in vitro* condition and it further spread
390 during clonal propagation. According to the network, kar1 would have generated -through
391 changes in somy of single chromosomes- a series of 'primary' derived karyotypes, (i) some
392 diverging early and being quite successful like kar2-4 and (ii) others having diverged later and/or
393 being less fit like the 19 minor karyotypes present around kar1. In this sense, there would be
394 secondary, tertiary waves of karyotype diversification, like kar5 emerging from kar2 and kar15
395 emerging from kar5. Time lapse single cell sequencing would be required to test this
396 hypothesis.

397 **Drug pressure and aneuploidy**

398 In cancer cells and in human pathogenic yeast, genetic diversity created by mosaic
399 aneuploidy has been linked to drug resistance[34,35]. In *Leishmania,* several *in vitro* studies report
400 whole chromosome somy changes as one of the first genetic changes in populations under drug
401 pressure[12,13,27,36,37]. However, it is still unknown if such variation in population average
402 aneuploidy is a reflect of a positive selection of a sub-population displaying a pre-existing
403 karyotype or is acquired *de novo* as a response to the pressure. The fact that the BPK282
404 population was previously used in *in vitro* drug selection experiments with at least 3 drugs[12,13,27]
405 allowed us to revisit the data of these experiments and compare the observed populational
406 aneuploidy pattern changes with single karyotypes identified by SCGS in the population in order
407 to address this question. In this context, we observed that the first contact of the parasites with
408 the drugs lead to the emergence of new 'populational karyotypes' that are similar to karyotypes
409 which were found in single-cells in the SCGS data (**Figure 5**). Thus, it seems that early stages of
410 aneuploidy changes are caused by selection of pre-existing karyotypes. However, further
411 exposure to higher concentrations led to somy changes that does not correspond to any
412 karyotype in our data. It is possible that these changes reflect selection of other, rarer
413 karyotypes that occur at frequencies lower than the detection limit of the droplet-based
414 method applied here. Nonetheless, since *Leishmania* is able to constitutively generate mosaic
415 aneuploidy[38], it is also possible that new karyotypes are generated *de novo* as a response to the
416 increasing challenge imposed by higher drugs concentration. Clonal lineages tracking methods,
417 such as DNA barcodes[39], should allow further insights in this matter.

418 **Conclusions**

419 In summary, this work represents the first description of complete karyotypes of individual
420 *Leishmania* parasites and open an unprecedent technological milestone to study MA in
421 trypanosomatids. Future work should focus on the emergence and evolution of MA during
422 clonal expansion by sequencing cells during very early stages of clonal evolution at different
423 timepoints, as well as following the dynamics of karyotype changes during different stages of
424 adaptation to drug pressure. Combining SCGS with single-cell transcriptomics could also allow
425 to understand better the impact of gene dosage imbalance on transcription with a single cell
426 resolution. Thus, high throughput single-cell sequencing methods represent a remarkable tool
427 to understand key aspects of *Leishmania* biology and adaptability.

428 **Figures:**

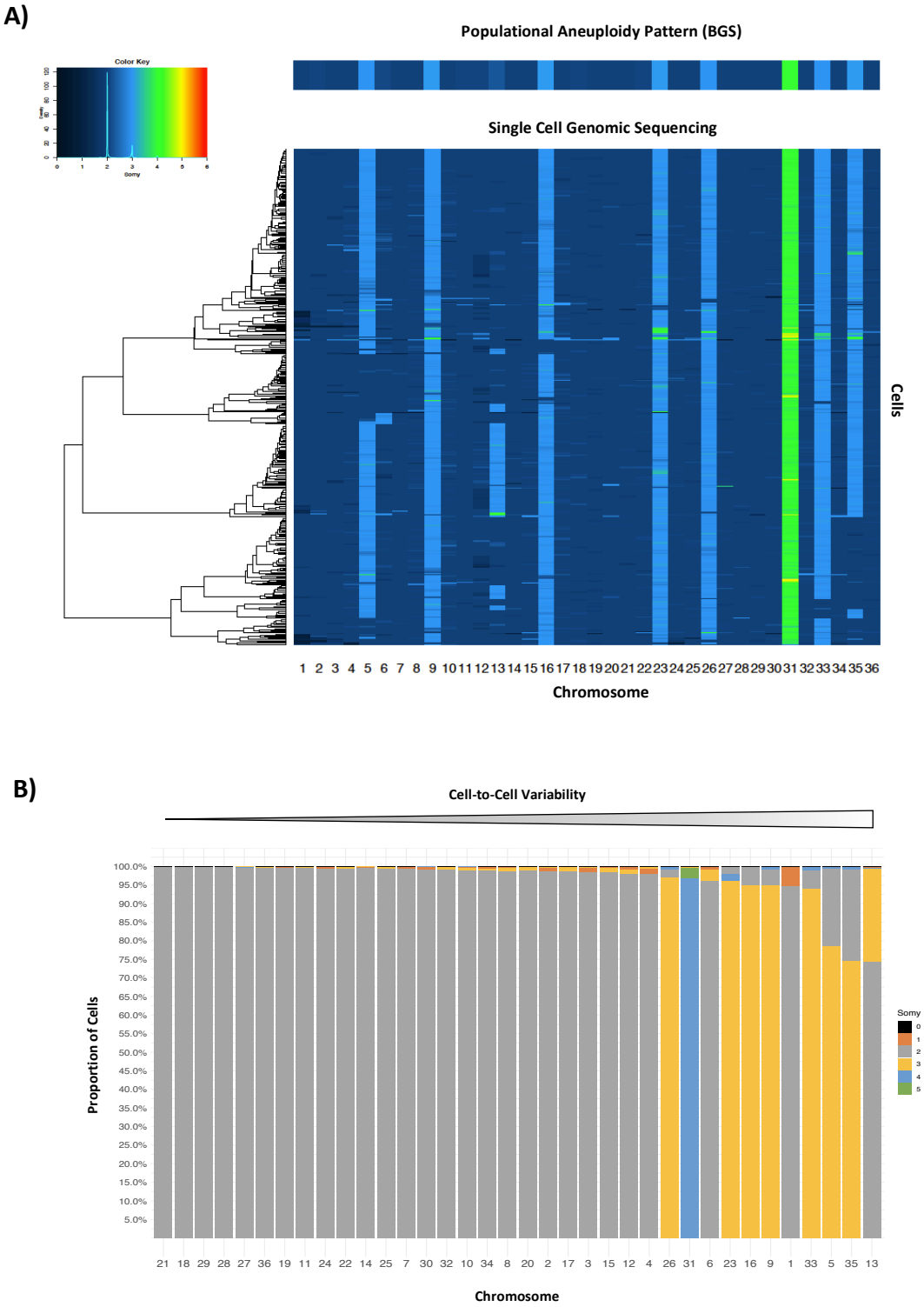

Figure 1 – **A)** Somy values of all 36 chromosomes of all 1560 cells in the BPK282 clonal population. The color key inset displays the distribution of somy values in the SCGS data. A heatmap based on BGS data of BPK282 is displayed on the top. **B)** Proportion of somies found for each chromosome. Chromosomes are arranged, from left to right, by cell-to-cell variability, defined as the proportion of cells displaying a somy different from the most frequent one. For each column, somy bars are stacked by the frequency they happen in the population.

429

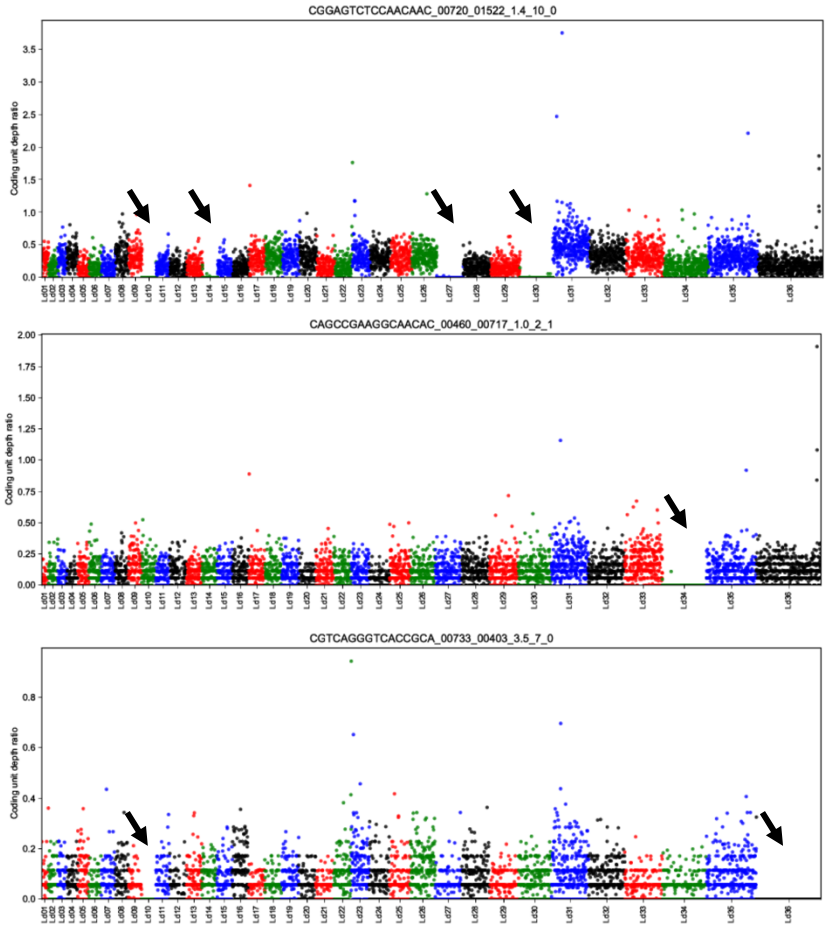

Figure 2 – Three examples of individual cells, identified by their 10X barcode sequence (top of each plot), where one or more chromosome is nullisomic. Manhattan plot displays average depth per 5kb. Nullisomic chromosomes are indicated with a black arrow. When present, single reads mapping to nullisomic chromosomes are reads composed by repetitive nucleotides that can be mapped to multiple regions of the genome.

A)

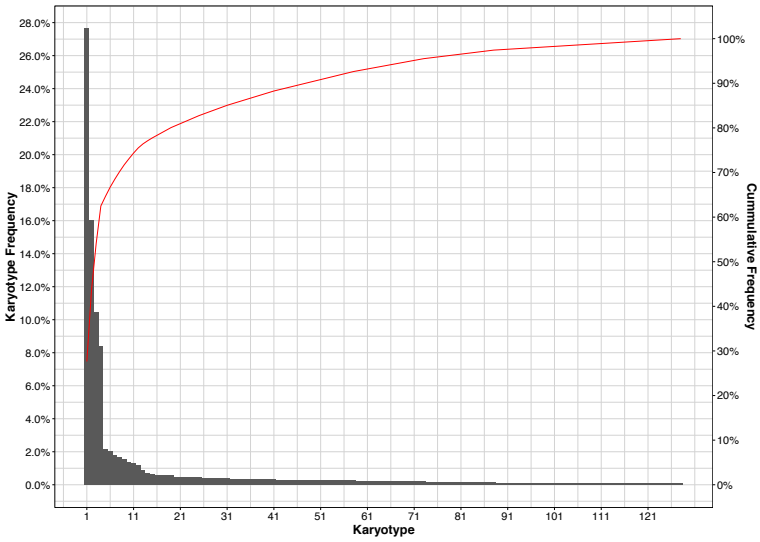

B)

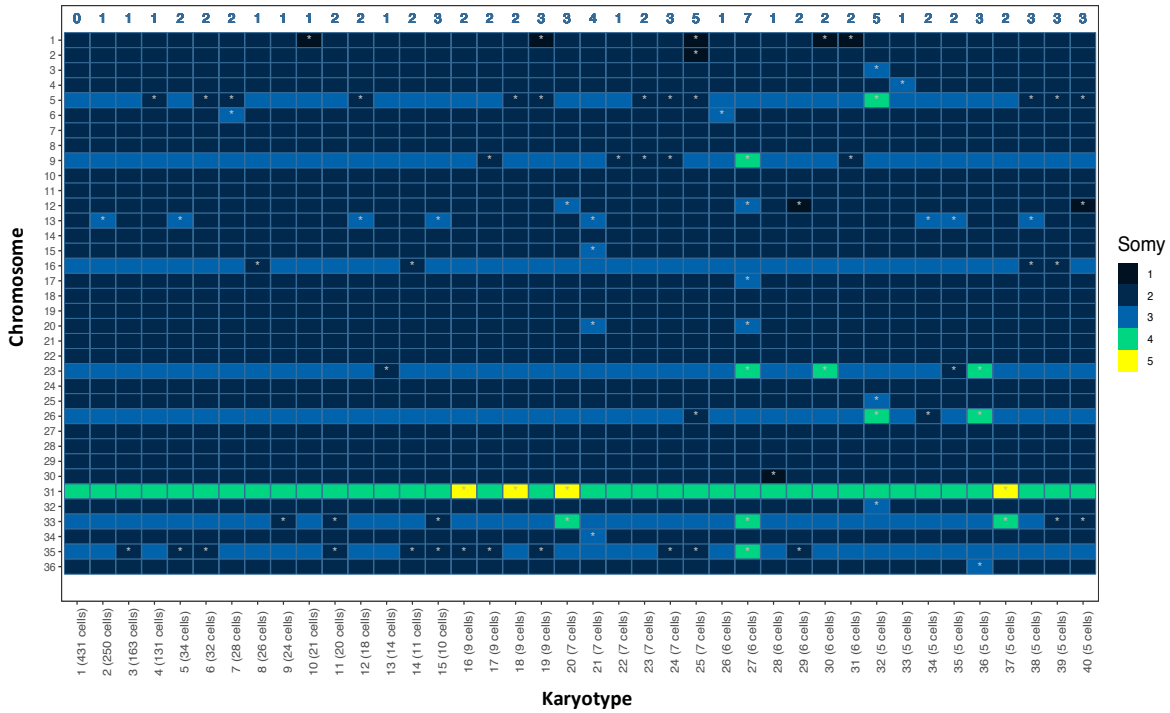

Figure 3 – Distribution and profile of different karyotypes identified among 1560 BPK282/0 cl4 promastigotes. **A)** Frequency distribution of all the 128 different karyotypes identified in the SCGS data. Red line indicates the cumulative frequency in the secondary axis. **B)** Heatmap displaying the somy values off each chromosome in the 40 most frequent karyotypes. Karyotypes are ordered from left to right and numbered according to their frequency in the population. Chromosomes in which somies diverge from the most frequent karyotype (Karyotype 1) are marked with a white asterisk. Blue numbers in the top part of the graph indicate the number of chromosomes with somy different from the first karyotype.

430

431

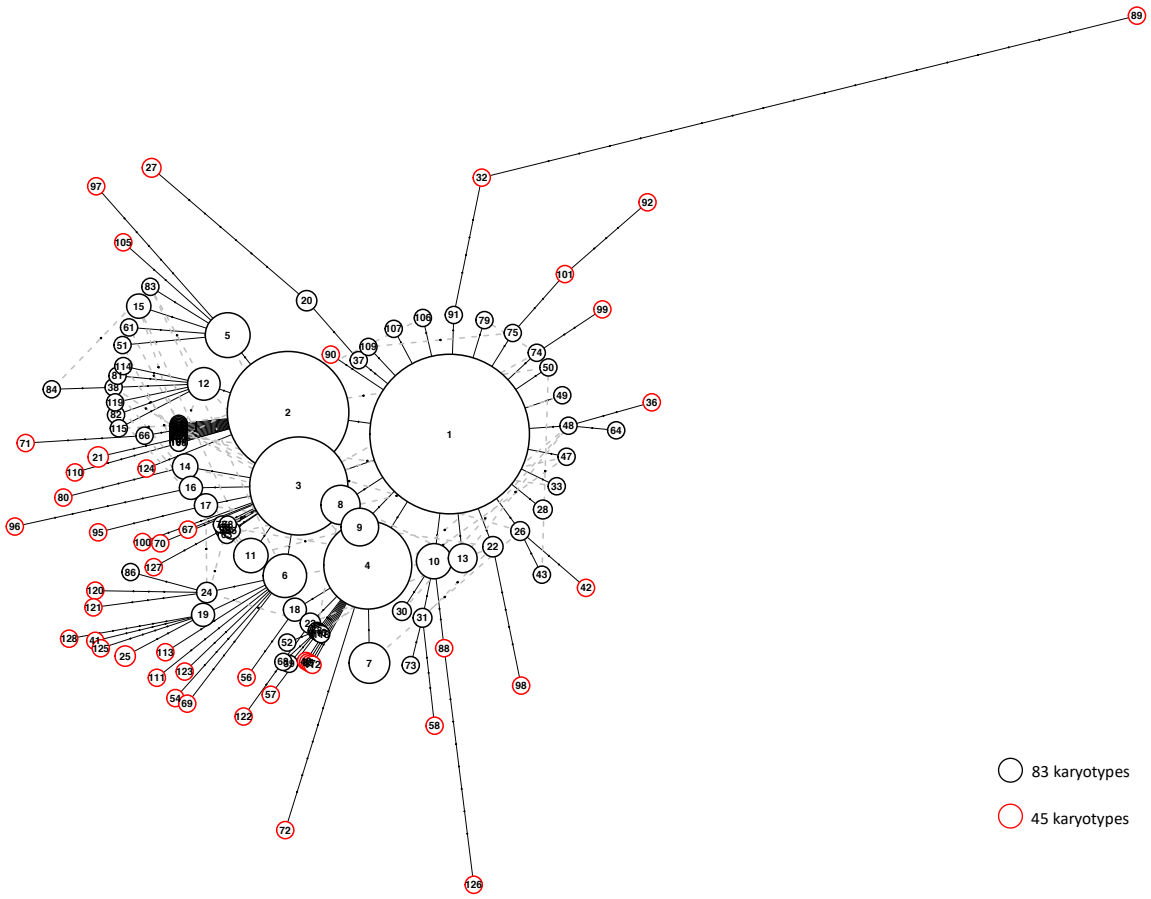

Figure 4 – Haplotype network between all 128 karyotypes. The dots in the link lines represent the number of different chromosomes between 2 karyotypes. Dashed grey lines indicate alternative links between karyotypes that diverge by a single chromosome (black pies). Red pies highlights karyotypes where the closest related karyotype display different somy in at least 2 chromosomes. The size of each pie is proportional to the number of cells displaying a given karyotype. The smallest pies represent a total of 7 or less cells.

432

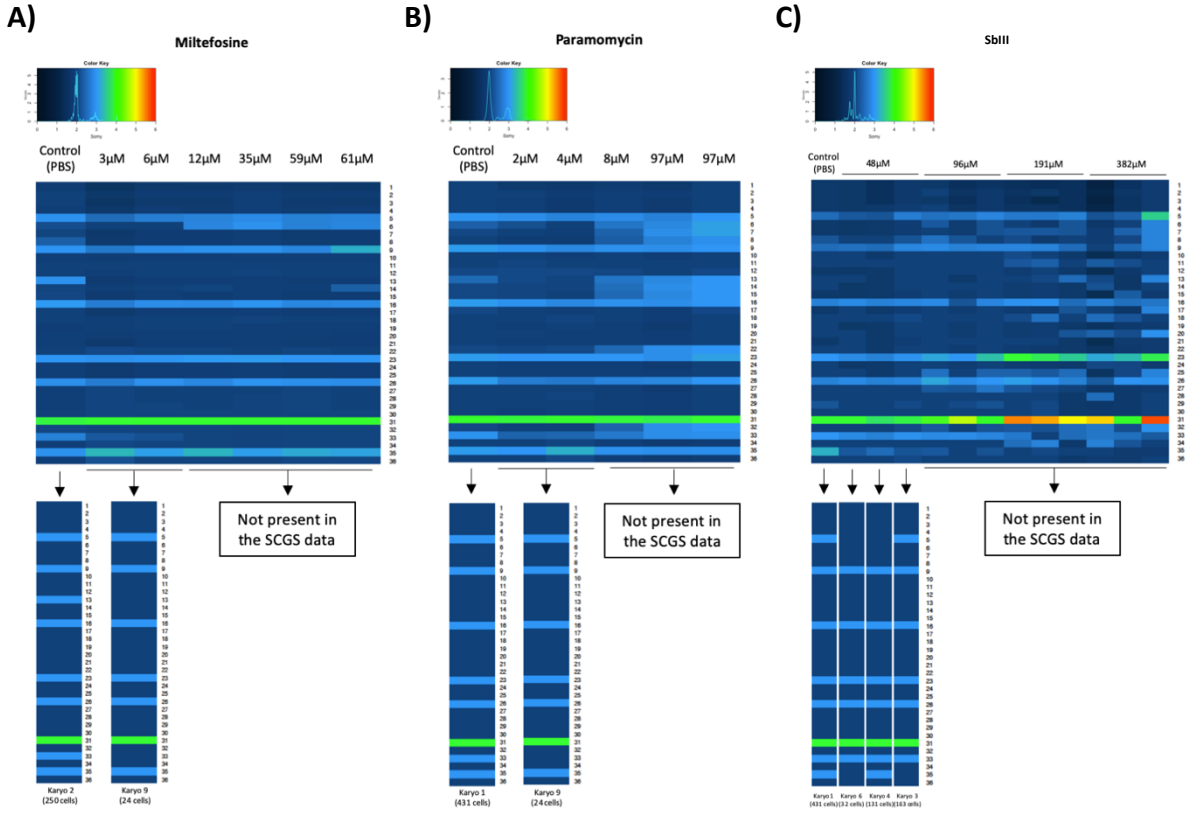

Figure 5 – Comparison between previously published somy estimation by BGS of BPK282/0cl4 strain during early adaptation to drug pressure (upper heatmaps) and individual karyotypes found in the SCGS data (bottom heatmaps). BGS somy values were published elsewhere for Miltefosine[13], Paramomycin[26] and SbIII[12].

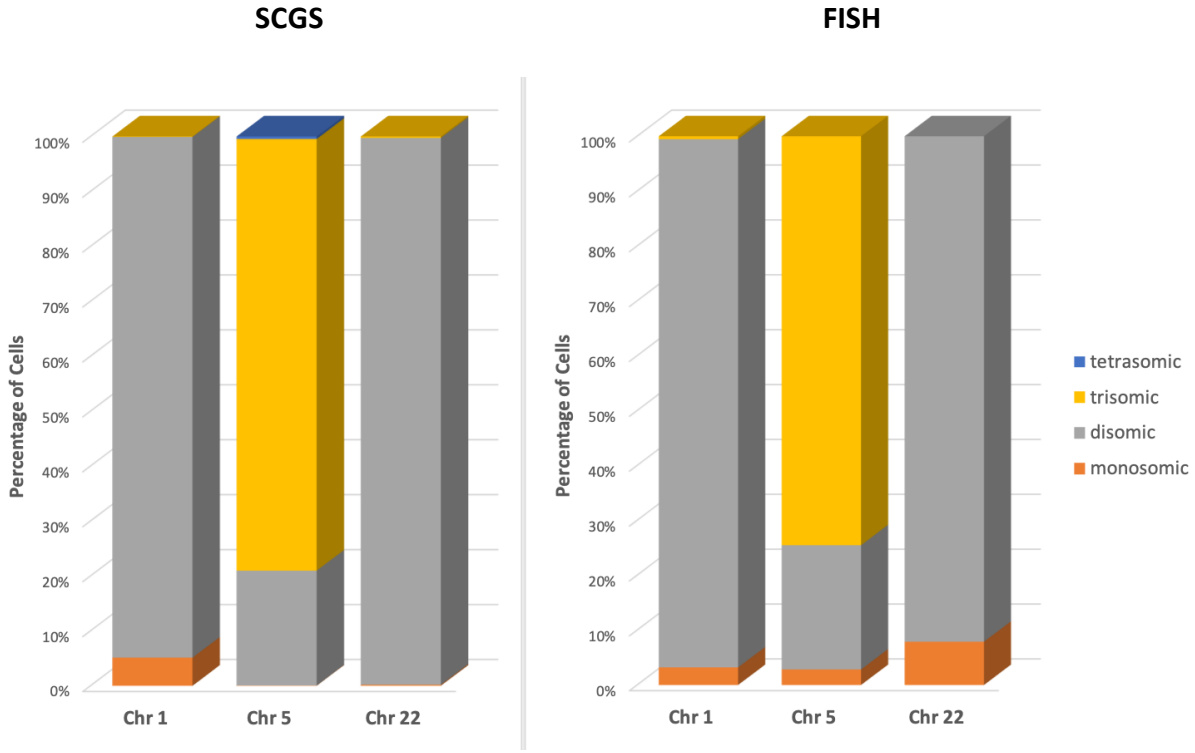

Figure 6 - Validation of the SCGS data using FISH. The proportions of cells displaying monosomic, disomic, trisomic and tetrasomic chromosomes 1, 5 and 22 were evaluated by FISH and compared to the same proportions found in the SCGS data.

436
437

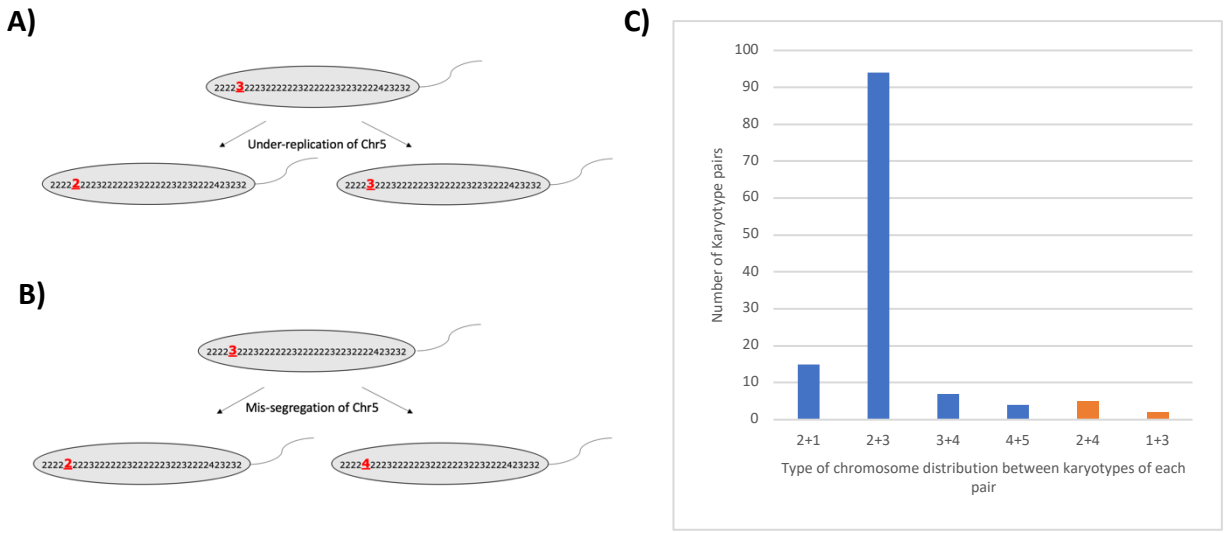

Figure 7 – Karyotypes found in the SCGS data support errors in chromosome replication during mitosis as main drivers of aneuploidy mosaicism. **A)** An example of an under-replication event that leads to two karyotype pairs displaying a "2+3" (odd) somy distribution in chromosome 5. **B)** A mis-segregation event in chromosome 5 would generate two karyotypes that display a "2+4" (even) somy distribution in the daughter cells. **C)** Karyotypes diverging by a single chromosome from the SCGS data were compared in pairs. The pattern of somies of the divergent chromosome in each pair is represented in the x axis. Odd patterns, representing putative under or over-replication events, are depicted in blue, while even patterns, a putative indication of mis-segregation events, are represented in orange.

Supplementary Material

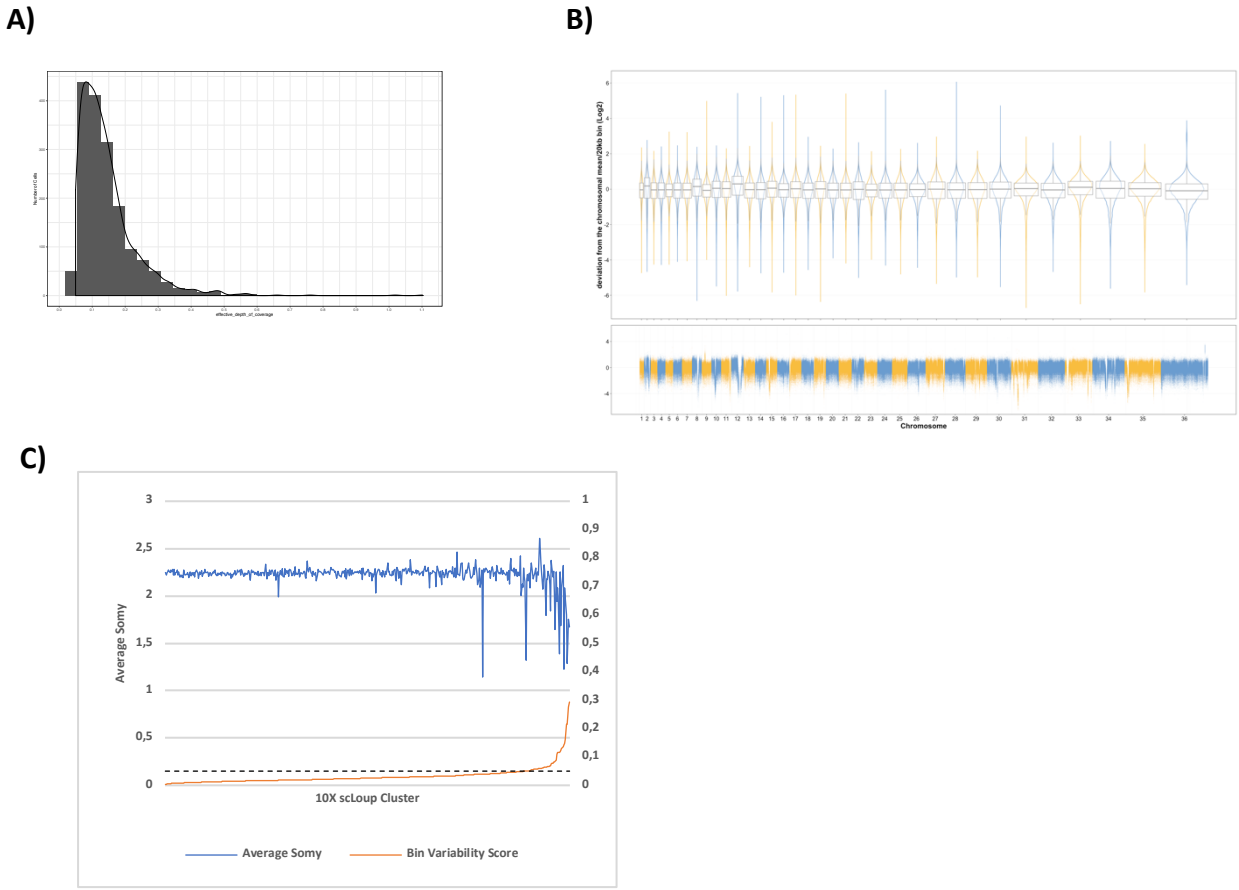

Figure S1 – A) Distribution of the effective coverage depth per cell. **B)** Violin plot showing the read depth deviation from the mean of intrachromosomal 20kb bins. For each cell, the mean depth/20kb of each chromosome was calculated and the ration between the depth of each intrachromosomal 20kb bin and the average was log2 transformed. Values close to 0 represent bins with depth similar to the chromosomal average. A box plot indicates the median (line in the center), the upper and lower quartiles (boxes) and the maximum and minimum of each chromosome (lines). A Manhattan plot on the bottom shows individual deviation values. **C)** Average somy and bin variability score of all 512 clusters. The black dashed line represents the threshold set to eliminate clusters with high bin-to-bin variability.

440

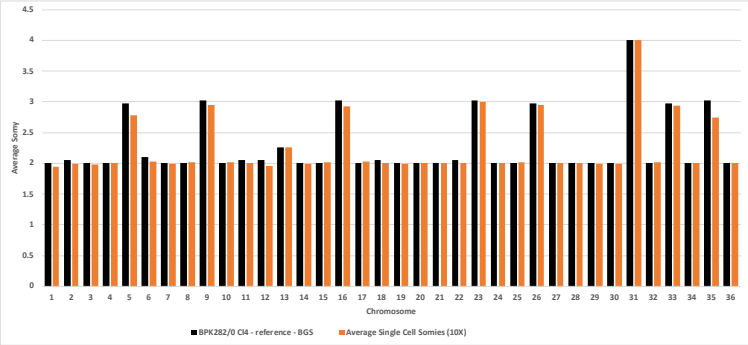

Figure S2 - Comparison of the average combined somy values of all 1560 BPK282/0 cl4 promastigotes assessed by SCGS (orange bars) with the average somies of a population of the reference BPK282 strain estimated by BGS (black bars).

441

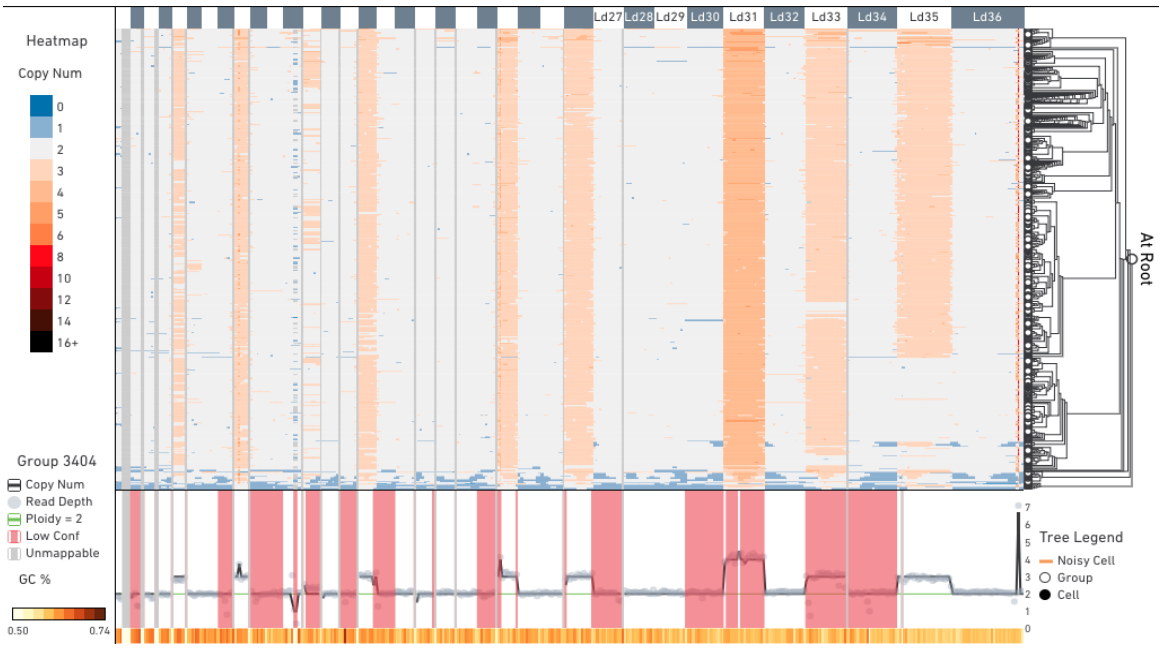

Figure S3 - CNV values calling by 10X Cell Ranger DNA pipeline visualized in 10X Loupe scDNA Browser tool. The 1703 cells are arranged in 512 clusters (horizontal lines). Bars on the top indicate the position of each chromosome, while lines and grey dots in the bottom represent the CNVs and reads/megabase, respectively, of all clusters combined. High copy number regions in chromosome 23 and 36 represent, respectively, the H-locus and the M-locus.

442

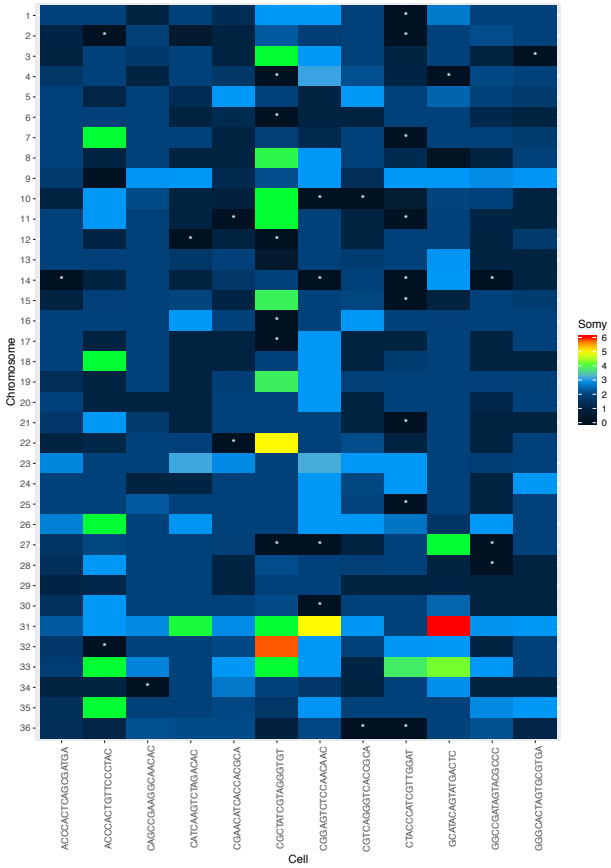

Figure S4 – Heatmap showing the estimated somy of all cells where at least one chromosome was missing, including cells removed from by data filtering. Nullisomic chromosomes are marked with a white asterisk.

443 **Bibliography**

444 1. Pelkmans, L. Cell Biology. Using cell-to-cell variability--a new era in molecular biology.
445 *Science* **336**, 425–6 (2012).

446 2. García-Betancur, J. C. & Lopez, D. Cell Heterogeneity in Staphylococcal Communities.
447 *Journal of Molecular Biology* (2019). doi:10.1016/j.jmb.2019.06.011

448 3. Gilchrist, C. & Stelkens, R. Aneuploidy in yeast: Segregation error or adaptation
449 mechanism? *Yeast* **36**, 525–539 (2019).

450 4. Seco-Hidalgo, V., Osuna, A. & Pablos, L. M. De. To bet or not to bet: deciphering cell to
451 cell variation in protozoan infections. *Trends Parasitol.* **31**, 350–356 (2015).

452 5. Burza, S., Croft, S. L. & Boelaert, M. Leishmaniasis. *Lancet* **392**, 951–970 (2018).

453 6. Adl, S. M. *et al.* The revised classification of eukaryotes HHS Public Access. *J. Eukaryot.*
454 *Microbiol Microbiol* **59**, 429–493 (2012).

455 7. Clayton, C. Regulation of gene expression in trypanosomatids: Living with polycistronic
456 transcription. *Open Biol.* **9**, (2019).

457 8. Reis-Cunha, J. L., Valdivia, H. O. & Bartholomeu, D. C. Gene and Chromosomal Copy
458 Number Variations as an Adaptive Mechanism Towards a Parasitic Lifestyle in
459 Trypanosomatids. *Curr. Genomics* **19**, 87–97 (2017).

460 9. Mannaert, A., Downing, T., Imamura, H. & Dujardin, J. C. Adaptive mechanisms in
461 pathogens: Universal aneuploidy in Leishmania. *Trends Parasitol.* **28**, 370–376 (2012).

462 10. Rogers, M. B. *et al.* Chromosome and gene copy number variation allow major structural
463 change between species and strains of Leishmania. *Genome Res.* **21**, 2129–2142 (2011).

464 11. Dumetz, F. *et al.* Modulation of aneuploidy in leishmania donovani during adaptation to
465 different in vitro and in vivo environments and its impact on gene expression. *MBio* **8**, 1–
466 14 (2017).

467 12. Dumetz, F. *et al.* Molecular Preadaptation to Antimony Resistance in *Leishmania*
468 *donovani* on the Indian Subcontinent. *mSphere* **3**, e00548-17 (2018).

469 13. Shaw, C. *et al.* In vitro selection of miltefosine resistance in promastigotes of Leishmania
470 donovani from Nepal: Genomic and metabolomic characterization. *Mol. Microbiol.* **99**,
471 1134–1148 (2016).

472 14. Cuypers, B. A systems biology approach for a comprehensive understanding of molecular
473 adaptation in *Leishmania donovani*. (University of Antwerp, 2018).

474 15. Sterkers, Y., Lachaud, L., Crobu, L., Bastien, P. & Pagès, M. FISH analysis reveals
475 aneuploidy and continual generation of chromosomal mosaicism in *Leishmania major*.
476 *Cell. Microbiol.* **13**, 274–283 (2011).

477 16. Sterkers, Y. *et al.* Novel insights into genome plasticity in Eukaryotes: Mosaic aneuploidy
478 in Leishmania. *Mol. Microbiol.* **86**, 15–23 (2012).

479 17. Barja, P. P. *et al.* Haplotype selection as an adaptive mechanism in the protozoan
480 pathogen *Leishmania donovani*. *Nat. Ecol. Evol.* **1**, 1961–1969 (2017).

481 18. Imamura, H. *et al.* Evaluation of whole genome amplification and bioinformatic methods
482 for the characterization of Leishmania genomes at a single cell level. *bioRxiv* (2020).

483 19. What is Cell Ranger? - Software - Single Cell Gene Expression - Official 10x Genomics
484 Support. Available at: https://support.10xgenomics.com/single-cell-
485 dna/software/pipelines/latest/what-is-cell-ranger-dna. (Accessed: 29th January 2020)

486 20. Single cell copy number calling -Software -Single Cell CNV -Official 10x Genomics Support.
487 Available at: https://support.10xgenomics.com/single-cell-
488 dna/software/pipelines/latest/algorithms/cnv_calling. (Accessed: 27th February 2020)

489 21. What is Loupe scDNA Browser? -Software -Single Cell CNV -Official 10x Genomics
490 Support. Available at: https://support.10xgenomics.com/single-cell-
491 dna/software/visualization/latest/what-is-loupe-scdna-browser. (Accessed: 29th
492 January 2020)

493 22. Clustering Cells -Software -Single Cell CNV -Official 10x Genomics Support. Available at:
494 https://support.10xgenomics.com/single-cell-
495 dna/software/pipelines/latest/algorithms/clustering. (Accessed: 6th February 2020)

496 23. Downing, T. *et al.* Whole genome sequencing of multiple Leishmania donovani clinical
497 isolates provides insights into population structure and mechanisms of drug resistance.
498 *Genome Res.* **21**, 2143–2156 (2011).

499 24. Paradis, E. Analysis of haplotype networks: The randomized minimum spanning tree
500 method. *Methods Ecol. Evol.* **9**, 1308–1317 (2018).

501 25. Paradis, E. Pegas: An R package for population genetics with an integrated-modular
502 approach. *Bioinformatics* **26**, 419–420 (2010).

503 26. Patino, L. H., Muñoz, M., Muskus, C., Méndez, C. & Ramírez, J. D. Intraspecific Genomic
504 Divergence and Minor Structural Variations in Leishmania (Viannia) panamensis. 1–19
505 (2020). doi:10.3390/genes11030252

506 27. Shaw, C. *et al.* Genomic and metabolomic polymorphism among experimentally selected
507 paromomycin-resistant Leishmania donovani strains. *Antimicrob. Agents Chemother.*
508 (2019). doi:10.1128/AAC.00904-19

509 28. Sterkers, Y., Crobu, L., Lachaud, L., Pagès, M. & Bastien, P. Parasexuality and mosaic
510 aneuploidy in Leishmania: Alternative genetics. *Trends Parasitol.* **30**, 429–435 (2014).

511 29. Hou, Y. *et al.* Comparison of variations detection between whole-genome amplification
512 methods used in single-cell resequencing. *Gigascience* **4**, 1–16 (2015).

513 30. Can I run non-human samples? – 10X Genomics. Available at:
514 https://kb.10xgenomics.com/hc/en-us/articles/360005055712-Can-I-run-non-human-
515 samples-. (Accessed: 5th February 2020)

516 31. Camacho, E. *et al.* Complete assembly of the *Leishmania donovani* (HU3 strain) genome
517 and transcriptome annotation. *Sci. Rep.* **9**, 1–15 (2019).

518 32. How much of a single cell's genome is amplified? – 10X Genomics. Available at:
519 https://kb.10xgenomics.com/hc/en-us/articles/360005108931-How-much-of-a-single-
520 cell-s-genome-is-amplified-. (Accessed: 6th February 2020)

521 33. Imamura, H. *et al.* Evolutionary genomics of epidemic visceral leishmaniasis in the Indian
522 subcontinent. *Elife* **5**, 1–39 (2016).

523 34. Sotillo, R., Schvartzman, J. M., Socci, N. D. & Benezra, R. Mad2-induced chromosome
524 instability leads to lung tumour relapse after oncogene withdrawal. *Nature* **464**, 436–440
525 (2010).

526 35. Selmecki, A. M., Dulmage, K., Cowen, L. E., Anderson, J. B. & Berman, J. Acquisition of
527 aneuploidy provides increased fitness during the evolution of antifungal drug resistance.
528 *PLoS Genet.* **5**, 1–16 (2009).

529 36. Rastrojo, A. *et al.* Genomic and transcriptomic alterations in *Leishmania donovani* lines

530 experimentally resistant to antileishmanial drugs. *Int. J. Parasitol. Drugs Drug Resist.* **8**,
531 246–264 (2018).

532 37. Patino, L. H. *et al.* Major changes in chromosomal somy, gene expression and gene
533 dosage driven by SbIII in Leishmania braziliensis and Leishmania panamensis. *Sci. Rep.* **9**,
534 9485 (2019).

535 38. Lachaud, L. *et al.* Constitutive mosaic aneuploidy is a unique genetic feature widespread
536 in the Leishmania genus. *Microbes Infect.* **16**, 61–66 (2014).

537 39. Blundell, J. R. & Levy, S. F. Beyond genome sequencing: lineage tracking with barcodes
538 to study the dynamics of evolution, infection, and cancer. *Genomics* **104**, 417–430 (2014).

539